Wire Less Sensors for Electromechanical Systems Diagnostics

Jinyeong Moon, *Member, IEEE*, and Steven B. Leeb, *Fellow, IEEE*

***Abstract*— The diagnostic machinery monitoring system presented in this paper coordinates the acquisition of vibration and speed estimates for an electric machine. It functions even when the machine is "off" or spinning down. This effectively turns the machine into its own mechanical network analyzer. Data from this system can be used to correlate electrical and mechanical data in order to distinguish a variety of pathologies in the machine and its mechanical mounts. The entire sensor system powers itself from surrounding magnetic fields, requiring no ohmic contact or special power wiring. The system presented in this paper presents a unique approach for fusing data from multiple sensors to create a coordinated picture of machine operation on a self-powered platform.**

***Index Terms*— Diagnostics, electromechanical, energy, harvesting, magnetic, saturation, self-powered, sensor.**

I. Introduction

USEFUL approaches to electromechanical systems diagnostics often involve the interpretation of health metrics developed from the data streams provided by multiple sensors of different types [3]. For example, instrumentation for measuring not only electrical consumption but also temperature might be deployed to develop useful metrics for determining the health of components, such as rotating machines and electrical protection gear. The approach of interpreting multiple streams of sensor data to develop a coordinated picture of machine health for fault detection and diagnostics is appealing. This approach could permit the scheduling of maintenance precisely at needed times, rather than performing unnecessary "scheduled" maintenance or waiting for a machine to fail [1], [2].

However, gathering useful information typically requires the installation of an expensive and intrusive array of sensors. The electronics advances that reduce the cost of individual sensors in an "IoT world" mask growing burdens. Sensor networks must be powered. Energy harvesting can reduce installation burden [4], [5]. Self-powered sensor nodes and energy harvesters are increasingly viewed as a convenient and feasible design technique for eliminating custom wired sensors [6]–[8]. A typical approach is to absorb energy from an environmental source, e.g., vibration, heat, or light, and to make measurements of an environmental parameter [11], [15]. Sometimes, the environmental source and parameter are the same [16], [17]. In other designs, a distinct energy source, e.g., a battery, may power a platform measuring a different environmental parameter [10], [18], [19].

A greater concern than simply powering sensors is the burden of developing useful information for supporting maintenance decisions from the sensed data. A sensor network may provide many colorful streams of data that can be stored and mined for information. However, the information must be collated, demanding a significant network bandwidth that grows as more "cheap" sensors are installed. Time synchronization must be maintained across data streams on different sensors to permit correlation and cross interpretation. Inexpensive sensors often do not automatically provide the actionable information necessary to validate the expense of the sensor installation.

This paper proposes a complete solution for providing actionable information from a collection of sensors installed with a minimum effort. This solution is demonstrated through an example sensor node, a vibration assessment monitoring point with integrated recovery of energy (VAMPIRE). The VAMPIRE uses a unique magnetic energy harvesting system with high power density relative to other harvesting methods, such as temperature [22] and vibration [23], without requiring any permanent magnet. The magnetic energy harvester can extract 120 mW with the surface area of 2.9 cm^2, whereas temperature and vibration energy harvesting typically require 1200 and 600 cm^2, respectively, for the same power level under realistic conditions. Electromagnetic energy harvesting is reliable and predictable compared with other harvesting techniques [24], [25]. This energy harvester is used to power a variety of different sensor packages, including vibration monitoring, current sensing, and temperature sensing. The sensor system uses stored energy from exposure to the machine's magnetic fields to power an efficient set of microcontrollers, power electronics, and magnetic field, electric field, and vibration sensors. The approach presented here avoids an excessive use of multiple, physically separate sensor nodes. It is a case study in coordinating multiple streams of information at a single sensor node with an integrated power electronic energy harvester to provide useful diagnostic and prognostic indicators.

This paper demonstrates a platform and an approach for fusing or correlating data from multiple different sensors to acquire a unique picture of electromechanical system health. Specifically, we consider monitoring rotating electric machines

Manuscript received October 16, 2017; revised February 7, 2018; accepted February 8, 2018. Date of publication March 29, 2018; date of current version August 9, 2018. *(Corresponding author: Jinyeong Moon.)*

J. Moon is with Maxim Integrated, North Chelmsford, MA 01863 USA (e-mail: jinmoon@mit.edu).

S. B. Leeb is with the Department of Electrical Engineering and Computer Science, Massachusetts Institute of Technology, Cambridge, MA 02139 USA (e-mail: sbleeb@mit.edu).

Color versions of one or more of the figures in this paper are available online at http://ieeexplore.ieee.org.

Digital Object Identifier 10.1109/TIM.2018.2814098

with a sensor package that powers itself from magnetic fields around the machine without requiring the presence of permanent magnets. When the electric machine is turned "OFF," it spins down with no connection to the electric utility. The multisensor VAMPIRE node can measure current with a magnetic field sensor, giving the sensor a precise time trigger when the machine is first deactivated. The sensor can also use an electric field sensor to measure a backelectromotive force generated by residual magnetic field trapped in the machine rotor, providing an estimate of the rotor speed during spin-down. A vibration sensor detects mechanical vibration in three axes during spin-down, and the temperature of the rotor can be recorded as well.

All of these capabilities are provided in a single installed sensor package about the size of a half dollar coin that becomes part of the terminal wiring box for the rotating machine. That is, the sensor package essentially "disappears" in the load and can be retrofit in existing machines. The sensor package replaces a 19-in rack filled with commercial monitoring equipment that would previously have been used to collect all of the relevant information recorded and analyzed by VAMPIRE. This paper compares new results from the VAMPIRE system with the expensive and bulky collection of commercial monitoring components. Specifically, this paper presents a first comparison of the VAMPIRE sensor approach to the vastly more expensive and bulky monitoring system that would have to be assembled from commercial monitoring components. Energy efficient implementations for wireless communication on multiple channels for control and data transfer are presented. The tiny VAMPIRE system provides results with the same fidelity as the commercial laboratory equipment, all in a single, easily installed package that requires no custom wiring for transmitting power or data.

II. Background

The VAMPIRE is a self-powered sensor node, specifically developed to detect early signs of certain pathologies of electromechanical systems. Magnetic energy harvesting with efficient power electronics permits the VAMPIRE to "fuse" sensor data from multiple sources and provide "actionable" information without the need for custom power wiring. Equally important, the VAMPIRE uses nonintrusive sensing of electric and magnetic fields to eliminate invasive sensors that require ohmic contact (voltage sensors) or mechanical connection (tachometer).

This section reviews the key subsystems of the VAMPIRE sensor package and sets the foundation for designing many different kinds of sensor packages using the energy available from a magnetic energy harvester.

A. Electromagnetic Energy Harvesting

The physical structure of an electromagnetic energy harvester begins with a 1:N current transformer [24], [26]. A single primary winding is provided by the current-carrying wire powering a device of interest, e.g., a motor. This wire passes through the center of a magnetic core, and a relatively higher number of turns, e.g., 200 turns in the example system, forms a secondary for energy harvesting and power processing circuitry. Unlike conventional current transformers, the magnetic core used for the energy harvester is operated into full magnetic saturation every cycle for maximum power extraction [24], [25]. The active use of magnetic saturation results in an unconventional selection of the magnetic core; energy extraction improves with a core with low hysteresis loss, high saturation flux density, and extremely high magnetic permeability [25]. The magnetic core selected for the VAMPIRE is an amorphous nanocrystalline core to provide these characteristics. In order to enhance energy extraction, the transfer window alignment (TWA) method [25] is employed in the VAMPIRE power package. This approach is resilient to changes in a primary current level. The TWA method carefully times power extraction and core saturation to achieve the maximum power extraction; a detailed analysis of the core modeling and the TWA method is presented in [25]. There is no physical ohmic contact between the primary side and the secondary side. The electromagnetic energy harvester is nonintrusive and can greatly simplify the wiring and power routing constraints, especially for a sensor application.

B. Spin-Down and Energy Buffer

Vibration measurements are most often performed in a steady-state operation. This is unfortunate. Machinery is designed to vibrate "least" under nominal operating conditions, and pathological situations may go undetected in a "normal operation" until pathologies, such as rotor imbalance, become extreme. The machine is more likely to expose problems during a spin-down as the machine passes through natural resonances. The harvester provides a unique opportunity for sensing, because the sensor can automatically detect the collapse of the magnetic field around the machine, indicating that the machine has been disconnected from the line. This observation marks the beginning of an opportunity to detect a spin-down vibration characteristic.

When the sensor package can be left *in situ* with its own reliable, rechargeable power supply, new sensing strategies can arise. The VAMPIRE harvests energy from magnetic fields created by the operation of the load under observation. As a side benefit, the VAMPIRE can also immediately determine when a load deactivates or disconnects from the utility. Because the VAMPIRE is self-powered, small, and therefore easily installed locally in a machine, e.g., in the motor terminal box, it can continue to monitor vibration and speed via back-EMF estimation as a machine "spins down." This "spin-down" event provides rich information regarding the health status of a motor and its mounting system. During a spin-down event, the rotor slows from full speed to a complete stop, analogous to a step change in the input of an electrical system. A frequency response obtained using the collected data during this noninvasive event can contain as much information in theory as a wide frequency sweep that mandates a complete control over an electromechanical system, e.g., exciting a motor at specific frequencies at specific times. Since a complete control cannot always be guaranteed (for example, a motor inside a military ship on

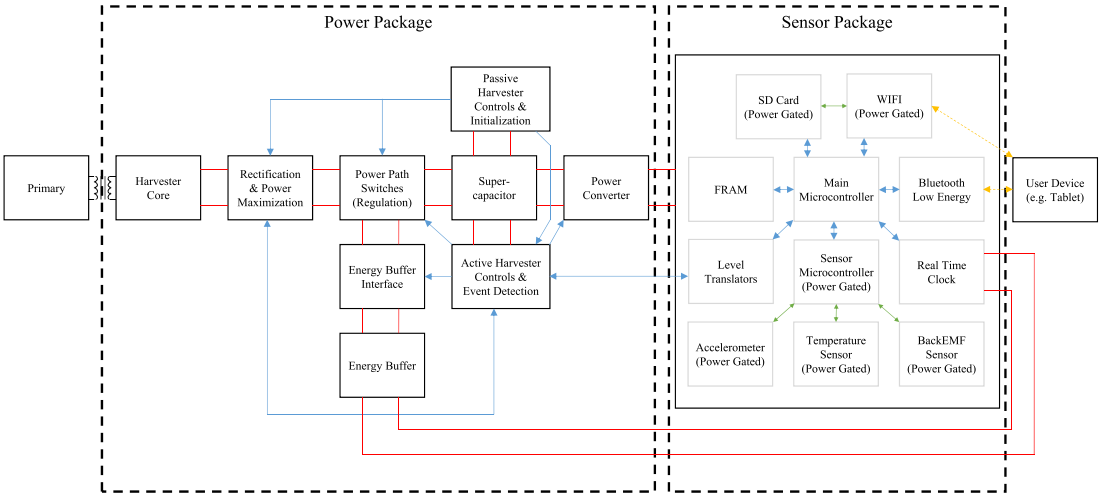

Fig. 1. Overall architecture of VAMPIRE.

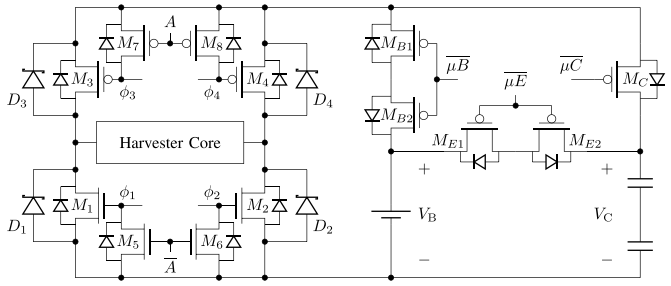

Fig. 2. Power path control circuit.

a live mission), noninvasive methods, such as spin-down analysis, are preferred. Moreover, as illustrated in [27, Fig. 8], a spin-down analysis can be comparable in terms of performance and accuracy to the invasive method as well.

Note that self-powered sensor packages offer an opportunity to collect information with potentially reduced need to penetrate environmental barriers with wires. The VAMPIRE contains an energy buffer to ensure continued operation while a machine cycles ON and OFF. The VAMPIRE can be integrated in the machine housing so that it is nonintrusive and quick to install.

Of course, the capacity of the main energy storage and the energy buffer must be appropriately selected. As the energy harvester inside the VAMPIRE heavily exploits magnetic saturation where the energy influx is limited to a narrow time window during a cycle, the main energy storage cannot be arbitrarily small. The capacity must be sufficiently large to provide sustenance during magnetic saturation. On the other hand, if the capacity of the main energy storage is exceedingly large, the initial "boot-up" time of the sensor node also becomes exceedingly long. For these reasons, the main energy storage is consisted of supercapacitors instead of small capacitors or Lithium polymer (LiPo) batteries. A higher capacity of the energy buffer is always beneficial as long as its physical size is not a limiting factor for the sensor node integration. In this embedded system, the energy buffer is a low-capacity LiPo battery with small physical dimensions.

C. Related Works

The promise of multisensor nodes for diagnostic applications has been recognized well over a decade [9]. References [18] and [20] discuss self-powered sensor nodes intended for motor diagnostics. However, these methods are physically invasive in nature as they fundamentally need to change the structure of a motor—a set of magnets need to be permanently attached to the shaft axle of a motor, unavoidably loading the electromechanical system. Aside from the mechanical loading, the energy harvesters introduced in these papers operate by mechanically spinning the said magnets as they are the source of changing magnetic fields, whereas the energy harvester introduced in this paper does not involve any physical movement, utilizing the magnetic fields emanating from the primary power line. Also, [18] and [20] assume that the entire electromechanical system can be fully manipulated by the sensor node as the rotational speed of the electromechanical system needs to be swept to get a set of frequency responses for analysis, whereas the VAMPIRE does not require any invasive control intervention as it only needs to collect naturally occurring data during a motor spin-down.

On the electromagnetic energy harvesting front, [11] captures power from ac power lines magnetically, but they are also based on vibration and permanent magnets. References [12] and [13] also discuss a similar objective of operating wireless sensor nodes with nonintrusive electromagnetic energy harvesters coupled with ac power lines. Reference [14] summarizes and compares in detail many electromagnetic energy harvesters for wireless sensor networks presented so far in the field. However, all these references require permanent magnets and associated vibration in order to work, and result in significantly less power level with a larger physical size due to permanent magnets and physical constraints.

III. Embedded System Architecture

The overall architecture of the VAMPIRE is presented in Fig. 1. The leftmost "Primary" block in Fig. 1 represents the electromechanical system, i.e., a motor, that the VAMPIRE is monitoring and extracting energy from. Through the

electromagnetic coupling formed by a magnetic core, given as the "Harvester Core" in Fig. 1, the magnetic energy is extracted and processed by the "Power" package, drawn in the dashed lines in Fig. 1 (left). The "Sensor" package, in Fig. 1 (right), operates with the power supplied by the "Power" package and communicates with a user device wirelessly.

A. Electromagnetic Energy Harvester

The primary side that carries the ac current and the energy harvester on the secondary side are electromagnetically coupled through a magnetic core. The harvested current from the core is generally a distorted nonlinear ac current, considering that the core experiences timed magnetic saturation every cycle. This distorted ac current goes through a power processing block, illustrated as "Rectification & Power Maximization" in Fig. 1. Two alternating sets of switches, M_1–M_4, in the detailed power circuit diagram (see Fig. 2) rectify the harvested ac current and at the same time maximize the power extraction from the core by performing the TWA technique [25].

In this energy harvester, an amorphous nanocrystalline core, VAC VITROPERM 500F W380, is used. The flux-shaping capacitor method [25] is not considered as the VAMPIRE is intended for a wide range of motor currents. The harvester core is wound 200 turns with an AWG23 wire. The AWG23 wire is selected such that it limits the parasitic flux accumulation [28] to be less than 10% of the total flux accumulation with the primary side current of up to $I_P = 100\ \mathrm{A_{RMS}}$, which is the maximum design target of the VAMPIRE.

This maximally harvested current is primarily stored in two supercapacitors connected in series, denoted as the "Supercapacitor" block in Fig. 1 and two capacitors in series in Fig. 2. The voltage rating of each supercapacitor (PAS0815) is 2.5 V and the capacitance is 1 F each. The nominal operating voltage for the power package is 4.0 V. This achieves $J = 0.8$ for the TWA method, which guarantees approximately 90.0% of the asymptotic maximum power [25].

When the energy harvester is operating, three paths are available for processing the extracted energy. The first path is to directly charge up the supercapacitors that power the sensor package. The second is to store the surplus energy into the energy buffer, shown as "Energy Buffer" block in Fig. 1, for sustenance during a spin-down event. The last path is to send the extracted current back to the primary side without dissipating it. As a self-powered system, a passive power flow is covered first.

B. Passive Control Phase

All the active paths that require active switchings, e.g., power maximization, regulation, and path controls, are disabled when the VAMPIRE boots up for the first time. In this passive stage, the unoptimized harvested current is steered to the "Supercapacitor" block through a full bridge diode rectifier, D_1–D_4. Body diodes of the FETs can be used without explicit Schottky diodes for simpler implementation with a higher loss. The voltage of the "Supercapacitor" block, V_C, increases at a slower rate due to the lack of active switching and the TWA method.

The voltage of the "Supercapacitor" block, V_C, is passively monitored all the time, using a hysteresis amplifier. $V_{\mathrm{Turn-on}}$ and $V_{\mathrm{Turn-off}}$ for the VAMPIRE are set to 1.98 and 1.90 V, respectively. The output of this hysteresis amplifier with $V_{\mathrm{Turn-ON}}$ of 1.98 V is directly used as the signal "A" in Fig. 1, implying "Active Control."

During this passive operation, another set of switches, M_5–M_8 in Fig. 2, initially bias the gates of the active switches with low quiescent current. These initial biasing switches are released at 2.07 V in this design. Beyond this point, the microcontroller provides active switching, dramatically improving energy extraction.

C. Active Control Phase

Until V_C reaches the nominal operating voltage of 4.0 V, the regulation and the power path controls are not required, and the first priority is to charge up the "Supercapacitor" block. With the TWA method and active rectification in place, V_C increases much faster, and once it goes beyond the nominal operating voltage of 4.0 V, the digital sensor package is powered ON. The sensor package has the hysteretic turn-ON and turn-OFF voltages of 4.1 and 3.85 V, respectively.

After the sensor package is turned ON, V_C is checked every line cycle for regulation. When it goes beyond 4.0 V, the harvester tries to regulate the voltage by rerouting the harvested current into other paths. The route is decided by checking the voltage of the energy buffer. In this embedded system, the energy buffer is a 220-mAh LiPo battery. LiPo batteries have much higher energy density than supercapacitors, much more suited for the size-constrained designs such as the VAMPIRE. If the voltage of the energy buffer, V_B, is less than its predefined maximum voltage, for example 4.20 V, the energy buffer receives the harvested current. In this cycle-based regulation, the upper bound for the maximum peak-to-peak ripple over a line cycle while charging V_C can be calculated by

$$\Delta V_{\mathrm{pp.chg}} = \frac{2}{C_{\mathrm{SUPERCAP}}} \cdot \int_{T/4-t_{\mathrm{SAT}}/2}^{T/4+t_{\mathrm{SAT}}/2} \frac{I_P}{N} \cdot \sin(\omega t) \quad (1)$$

where

$$t_{\mathrm{SAT}} = \frac{2\, B_{\mathrm{SAT}}\, A_{\mathrm{CORE}}\, N}{V_{\mathrm{C}}}. \quad (2)$$

With $C_{\mathrm{SUPERCAP}} = 0.5$ F, freq $= 60$ Hz, $V_{\mathrm{C}} = 4.0\ V$, $N = 200$, $B_{\mathrm{SAT}} = 1.19$ T, and $A_{\mathrm{CORE}} = 36\ \mathrm{mm}^2$, the charging ripple is $\Delta V_{\mathrm{pp.chg}} = 10.84$ mV with $I_P = 100\ \mathrm{A_{RMS}}$. The maximum voltage ripple over a line cycle while discharging V_C without the harvested current can be calculated by

$$\Delta V_{\mathrm{pp.dis}} = \frac{I_{\mathrm{LOAD}}}{C_{\mathrm{SUPERCAP}} \cdot \mathrm{freq}} + I_{\mathrm{LOAD}} \cdot R_{\mathrm{ESR}}. \quad (3)$$

With $I_{\mathrm{LOAD}} = 10$ mA for the sensor package and R_{ESR} of 140 mΩ for the two supercapacitors in series, $\Delta V_{\mathrm{pp.dis}} = 1.733$ mV. Therefore, the VAMPIRE achieves V_C regulation with the maximum peak-to-peak ripple of approximately

11 mV at the nominal operating voltage of 4.0 V and the maximum primary current of 100 A_{RMS}.

The energy stored in the energy buffer will be used later for spin-down events and wireless data communication. The energy buffer must be used with a strict rule: the net energy into the buffer must be nonnegative between operations as this is a self-powered embedded system. As long as the nonnegative energy flow can be guaranteed, a higher energy capacity is preferred for the energy buffer as it can increase the operating time of the embedded system. This is why a LiPo battery is favored over supercapacitors for the energy buffer. As will be introduced later, 200 mA is the current approximately required for sustaining the WIFI module inside the sensor package. To sustain this level of current for a 30-s-long wireless communication, more than 40 F is required for a voltage drop of less than 150 mV. This implies the use of more than 80 supercapacitors, potentially unattractive for a volume-constrained sensor node application.

The main energy storage, "Supercapacitor," on the other hand, cannot be swapped with a LiPo battery for a longer operation time, because the time to charge up the main energy storage to boot up the system would take a significantly longer time. For the main energy storage, the voltage ripple, which is negligible, is traded off with a fast boot time.

When both the supercapacitor block and the energy buffer are at their maximum voltage, the harvested current is rerouted back to the primary side without experiencing any voltage drop by shorting the secondary side terminals of the core. When the secondary side of the current transformer is shorted, the primary side effectively becomes a wire, resulting in negligible loss from the secondary side. The lower nFETs, M_1 and M_2, are both turned ON to provide a short-circuit path for the core. At the same time, the upper pFETs, M_3 and M_4, are turned OFF at the same time to isolate the energy storages.

Since there are two different energy sources with potentially different voltage levels in general, the pFETs in the power processing circuits are controlled by the highest voltage existing in the circuit with the shared ground.

In the electromagnetic energy harvester, the LiPo charging circuit can be as simple as two switches, M_{B1} and M_{B2} in Fig. 2, as the core serves as a current source. For the VAMPIRE, a 220-mAh LiPo battery with the maximum charging rate of 2 C is chosen. It is small enough to be easily enclosed inside the VAMPIRE structure, and it can withstand the primary side current up to 97.7 A_{RMS} to be under its 2-C rating with $N = 200$. The maximum primary current for a battery capacity is calculated by

$$I_{P-\mathrm{RMS}} = \frac{2\,\mathrm{Capacity} \times N}{\sqrt{2}} \cdot \frac{\pi}{2}. \tag{4}$$

The constraint 97.7 A_{RMS} also closely match the 100 A_{RMS} limitation for the wire gauage calculation.

D. Spin-Down Event Detection

The harvester core is essentially a current source while it is not saturated, developing any voltage that is required to sustain a current path into the load. Therefore, the core voltage is instantly developed to the full load voltage whenever the load current exists. By monitoring the terminal voltages of the core as digital signals, the harvester microcontroller can easily determine the direction of the current, as well as the location of the zero crossings of the primary side current. Using passive rectification, a zero crossing coincides with a rising edge in either terminal voltages. As the TWA method can potentially obscure the location of a zero crossing, however, the VAMPIRE employs a zero crossing training every cycle [21]. As soon as the harvester microcontroller obtains the location of the most recent zero crossing, it estimates the location of the transfer window and the location of the next zero crossing based on the previous history. If the next zero crossing is not detected at this estimated time window within some margin, it indicates that the primary side has lost its electrical power to sustain magnetic fields, and an indication of the initiation of the spin-down event is sent to the sensor package.

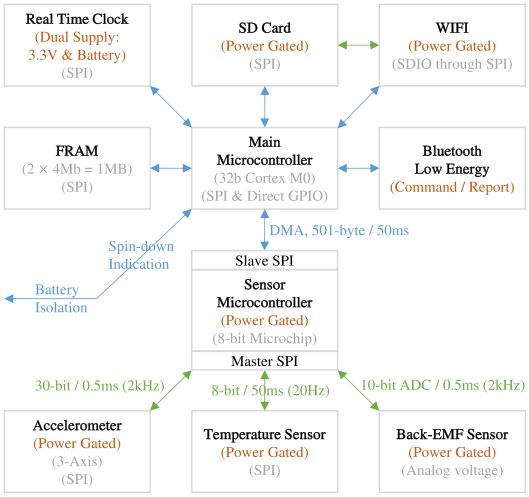

Fig. 3. Sensor package block diagram.

IV. Sensor and Wireless Communication Package

A. Sensors and Data Reports

The accelerometer and the back-EMF sensor are sampled at 2 kHz, and the temperature is sampled at 20 Hz. They are all connected in serial peripheral interface (SPI) as slaves to the sensor microcontroller. The sensor microcontroller and the sensors can be power gated for lower power consumption. Relative vibrational energy can be inferred from the acceleration data collected from the accelerometer. The back-EMF sensor measures the back-EMF voltage appearing across the phase wires of the motor by capacitive coupling during a motor spin-down, and the rotational speed of the motor can be inferred from this data. More detailed illustration of the sensor package is presented in Fig. 3.

The accelerometer IC, BMA250E, reports three-axis acceleration data, each axis in 10-bit resolution. The back-EMF sensor generates an analog voltage and is sampled with a 10-bit analog-to-digital converter (ADC) inside the sensor microcontroller. Combining these sensor reports, a fast sample packet of 5 B (40 bits) is constructed at 2 kHz. The temperature sensor reports 8-bit data, and for every 100 fast sample

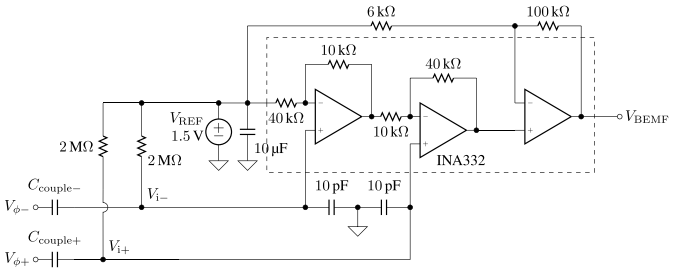

Fig. 4. Back-EMF voltage sensor circuit.

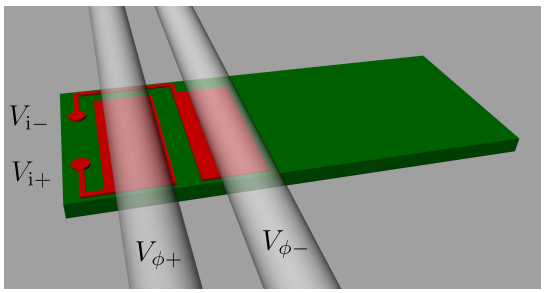

Fig. 5. Back-EMF voltage sensing structure.

packets, 1 B (8 bit) of temperature data are added to the data collection. The sensor microcontroller has two SPI buses. In one SPI bus, it acts as a master and controls various sensors. In the second SPI bus, it acts as a slave and it is controlled by the main microcontroller. The separation of sampling layer effectively transforms a low bandwidth constant data flow to a higher bandwidth sparse input.

B. Autonomous Data Flow

The main microcontroller immediately writes the received data into the ferroelectric random access memory (FRAM) block that consists of two 4-Mb FRAM modules that are all connected in SPI as slaves to the main microcontroller. Data of 8-Mb allow writing of approximately 100 s worth of data samples. The FRAM block is written in a ring fashion, overwriting the oldest data. Once a spin-down event is finished, the entire 100 s of recording is transferred to the more permanent and spacious SD card. The SD card is also connected in the SPI as a slave to the main microcontroller, and it is power gated as it consumes a relatively high amount of power compared with other sensors and microcontrollers. The file system for the SD card is FAT32, and currently 150 data files are supported in the embedded system. The time stamp for each file is acquired by querying the real-time clock connected in the SPI. The SD card is required in the design, because an FRAM module is extremely limited in data storage capacity compared with its physical size. However, the FRAM modules are also essential in the design, because the SD card consumes much higher power than FRAM modules, and the SD card is inappropriate for constant low-latency writings, which eventually necessitates an additional data buffer layer, such as FRAM and SRAM.

C. Back-EMF Voltage Sensor Design

The schematics for the back-EMF voltage sensor are presented in Fig. 4. The copper deposits on the printed circuit board (PCB), as shown in Fig. 5, serve as bottom plates of the capacitors, and the phase wires above them, $V_{\phi+}$ and $V_{\phi-}$, act as top plates of the capacitors. Two capacitors designated as $C_{\text{couple}+}$ and $C_{\text{couple}-}$ in Fig. 4 represent these voltage sensing capacitors. The capacitively coupled phase voltages then go through differential amplifiers. Due to the capacitive input to the amplifiers' positive terminals, a differentiator is inherently implied. The gain of the amplifier is set sufficiently high that the output is clipped to the rail voltages most of the time. The speed of the rotor can still be estimated by tracking the zero crossings in the back-EMF voltage, instead of performing a Hilbert transform on the nonclipped decay of the sinusoidal voltage waveform [27]. These two reasons—implying a differentiator and tracking only zero crossings instead of voltage envelopes—severely limit us to directly compare and overlay the raw ADC readings of the back-EMF sensor in the VAMPIRE with raw data acquired by commercial probes both in the locations of the zero crossings and signal scale. However, the performance of the entire sensor suite, including the back-EMF sensor, is sufficiently accurate to provide a capability of discerning pathologies as will be illustrated in Section VI. This implementation is consisted of low-power amplifiers and a low-power voltage reference to bias the inputs and outputs of the amplifiers. Unlike the back-EMF design introduced in [29], which requires a high amount of current to operate (around 10 mA), this voltage sensor can be operated with less than 1 mA. The supply voltage to the back-EMF sensor is 3.3 V.

D. Spin-Down Event Autotrigger

During a spin-down event, high power consumption is soon expected for the SD card writing. Therefore, the energy buffer must be connected to prevent the "Supercapacitor" block from overly discharged. The harvester microcontroller will automatically provide a current path between the "Energy Buffer" and the "Supercapacitor" blocks upon the detection of a spin-down event.

Querying the sensors and storing the data into the FRAM block are further continued for a prespecified duration as a spin-down may take up to tens of seconds. When the end of the spin-down is reached, the main microcontroller is fully committed to finishing the data transfer between the FRAM and the SD card. After the spin-down event is recorded as a file in the SD card, the real-time clock is queried, and the time-stamp is also stored. Then, the harvester microcontroller goes into the state where it looks for a rising edge in either of the core terminals to detect the primary turn-ON again.

E. Wireless Communication

The VAMPIRE supports Bluetooth Low Energy (BLE) and WIFI. As the BLE is specialized in low-power and low-bandwidth communication, the BLE connection for the VAMPIRE is primarily used for issuing commands. The actual

TABLE I
BLE CHARACTERISTICS

BLE Characteristics	Address	Remark
Command Input from User	h'9F3F	Refer to BLE Command*
File Table	h'9F40	MSB: Most Recent Slot Number Otherwise: Each Bit = Slot Written
Power Table	h'9F41	Refer to BLE Command*
Current Sensor Value Report	h'9F42	AccMSB X/Y/Z, BEMF, AccLSB, T
Status Report	h'9F43	Energy Buffer Voltage (h'03FF) Spindown Indication (h'1) Record (Future) Indication (h'1) Powersave Mode Indication (h'1) Primary On Indication (h'1)
BLE Connection Parameters Report	h'9F44	Connection Interval (h'FFFF) Connection Timeout (h'FFFF) Connection Latency (h'FFFF)
RTC Report	h'9F45	Y/M/D/H/M/S

TABLE II
BLE COMMANDS

BLE Command*	Cmd Hex	Remark
Power Gating Config (Power Table*)	h'01xx	Sensor(5), SD(3), WIFI(1)
		Persist(7), Energy Buffer(0)
File Slot Deletion	h'02xxyy	Delete One Slot xx = 01 – 96
		Reset Table: xx = 00, yy = FF
Current Sensor Value Checkup	h'030x	On/Off: x = 1/0
Record 100s from now	h'040x	On/Off: x = 1/0
Record the most recent 100s til now	h'050x	On/Off: x = 1/0
BLE GATT Force Disconnect	h'06	
WIFI Module SSID/Password	h'07xxY[8]	SSID = xx, Y[8] = 8 Byte PW
Retrieve RTC	h'08	
Set RTC	h'09Y[6]	Y[6] = Y/M/D/H/M/S

transmission of collected raw data is handed off to the WIFI module, as energy per file download is comparable in the case of one file, and significantly less if two or more files are transferred. Though the data files can generally be downloaded at a far greater rate with the WIFI, note that the WIFI connection is very costly in terms of power, and the connection can be weakened by distance and obstacles between the WIFI module and the data receiver.

The BLE connection can be made to the VAMPIRE any time. The BLE module maintains multiple characteristics as described in Table I, and the BLE command structure is described in Table II. The WIFI connection can be made upon user's request through the BLE and must be closely controlled by the user as it is a power-intensive operation.

Once a spin-down event is completed, the most likely scenario for a service staff is to make a BLE connection to the VAMPIRE and check the recently stored file table by checking the second BLE characteristic (h′9F40). If there is a new data file, the staff will issue a command to turn ON the WIFI module and download the file through the WIFI connection. When the WIFI module is turned ON by a BLE command, the WIFI module internally initializes an http server, which takes approximately 20 s to be ready for data transfer. As the WIFI module in the VAMPIRE supports IEEE 802.11b/g/n, each file transfer finishes almost instantly. The staff will then turn OFF the WIFI connection and disconnect the energy buffer from the "Supercapacitor" block to completely turn OFF the VAMPIRE until the next run.

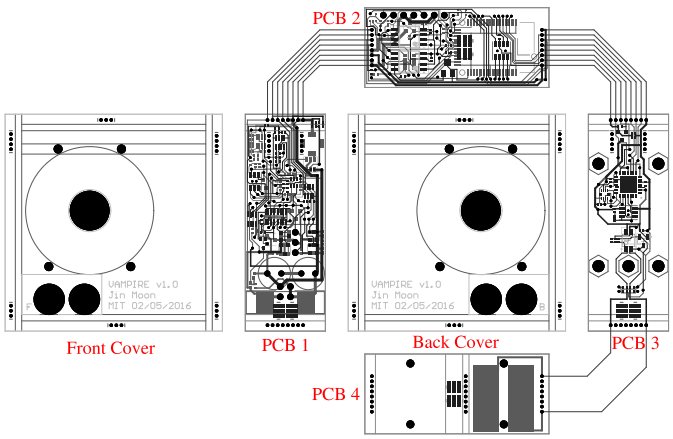

Fig. 6. VAMPIRE PCBs layout.

The main microcontroller is in fact a relatively powerful processor (32-bit ARM Cortex M0 CPU) inside the BLE module. As it is always ON for user communication, it doubles as a main microcontroller and as a BLE stack handler to save power and space. The WIFI module is packaged together with the SD card (Toshiba FlashAir). The WIFI module can be accessed by software through intelligent secure digital input output standards. When the WIFI module and the SD card are actively power gated, all their relevant SPI pins must be tristated.

V. PHYSICAL CONSTRUCTION

The physical structure of the VAMPIRE is based on the PCBs. The layout of the entire PCBs is presented in Fig. 6. Six PCBs are used as six faces to create a rectangular box, and joints between neighboring PCBs are formed by soldering board-to-board pins or using socket-plug pairs. The inner frame is formed by four narrow PCBs. This rectangular structure is soldered with rows of 90°, 0.5-mm pitch male pins. These soldering connections provide both physical structure integrity and electrical signal connection between two neighboring boards. In order to provide a firm and stiff environment for the accelerometer, the mounts which the VAMPIRE uses to attach itself to the motor cover are directly placed on the sensor board, which are emphasized by hexagonal shapes in "PCB 3." The front and back covers do not have any electrical connection. They provide physical protection for the four boards on side faces. The structure is designed such that all the outside faces of the PCBs are protected by the raised walls from neighboring PCBs. The height of the raised wall is calculated based on the tallest component in the entire design, which is 2.5 mm.

The magnetic core is placed inside of this box structure. The location of the core is marked on the front and back covers. The wire that goes through the center of the core for energy harvesting can also serve as one of the two phase wires for the back-EMF voltage sensor. Two supercapacitors for the "Supercapacitor" block and the 220-mAh LiPo battery of the "Energy Buffer" block are placed inside of this structure as well. The VAMPIRE prototype before permanently affixing

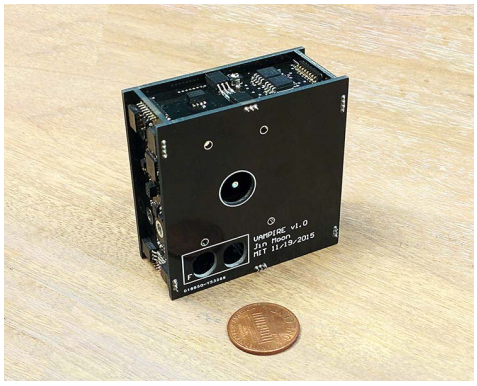

Fig. 7. VAMPIRE prototype.

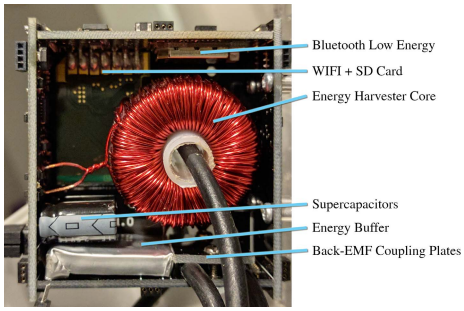

Fig. 8. VAMPIRE prototype internal.

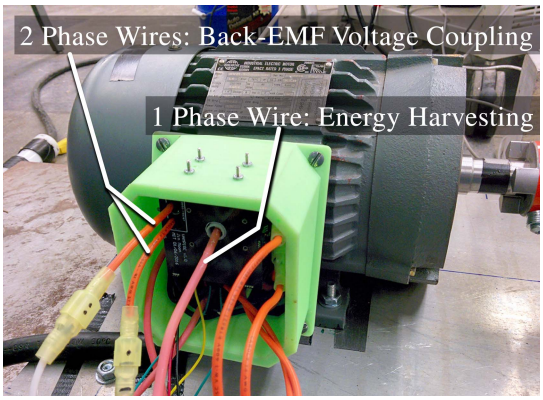

Fig. 9. VAMPIRE in the experimental setup.

the magnetic core inside is presented in Fig. 7 and compared against the U.S. one cent coin. The detailed internal structure with the mounted core is presented in Fig. 8. The core is strongly affixed to the structure by the inner cylinder and the adhesives on the front and the back.

VI. Experiment

A. Experimental Setup

The VAMPIRE is installed in a real vibration testing setup as shown in Figs. 9–11. The bright green cover for motor's terminal box is 3-D printed to provide a secure mount for the VAMPIRE, replacing the existing external cover. This retrofit installation of the VAMPIRE replaces all the equipment required for sensing, data storage, and communication

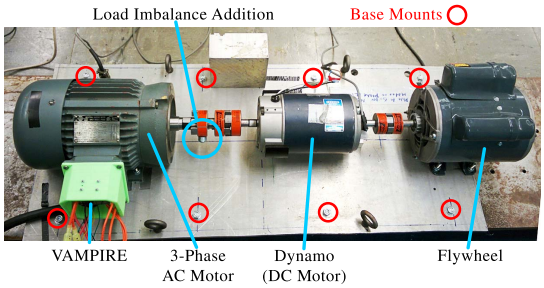

Fig. 10. Experimental setup—electromechanical system.

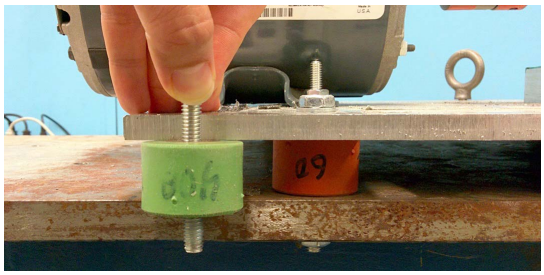

Fig. 11. Experimental setup—base mounts with changeable stiffness.

in [27] to generate an empirical vibrational transfer function (eVTF [27]), based on a second-order spring-mass-damper mechanical system [31], [32]. The replaced components are commercial off-the-shelf accelerometers, standalone back-EMF sensors, data acquisition blocks, data storage, wireless network capability, and power supply and wiring.

In this experiment, the VAMPIRE harvests energy from one of the three phase wires of the ac motor and provides health information of the electromechanical system (the motor and the mechanical load attached to the motor). In Fig. 9, one phase wire in the center feeds magnetic fields to the magnetic core inside the embedded system. This wire and one additional phase wire are capacitively coupled to provide a differential voltage input to the back-EMF sensor. Though Fig. 9 shows test wirings outside the cover for debug and measurement purposes, wirings can be completely contained inside the green cover and the front face of the cover can be sealed in real applications. Also, one of the phase wires used for the back-EMF voltage coupling in Fig. 9 is the same wire used for energy harvesting, making the total number of required phase wires two. In an ideal condition, only one phase wire is sufficient for harvesting energy and extracting speed information from the back-EMF voltage sensor. However, due to the physical proximity to other phase wires inside a small terminal box, rejection of common-mode voltage coupling using more phase wires greatly increases the accuracy of the back-EMF voltage sensor. In our experiment with the control box of a 1.5-hp motor, two phase wires were chosen based on the sensor accuracy and wiring complexity.

Once the electromagnetic energy harvester powers up the entire embedded system, the motor is abruptly turned OFF to create a spin-down event. The VAMPIRE is accessed via BLE connection, and the internal WIFI module is enabled. The stored raw data files which contain the collected sensor

TABLE III
POWER CONSUMPTION

Block	Current	Voltage	Power Consumption
Harvester Microcontroller	1.3mA	4.0V	5.20mW
Sensor Microcontroller	3.9mA	3.3V	12.9mW
Accelerometer + Temperature	0.15mA	3.3V	0.495mW
Back-EMF Sensor	0.85mA	3.3V	2.81mW
Main Microcontroller + BLE	3.6mA	3.3V	11.9mW
FRAM	1.5mA	3.3V	4.95mW
Real Time Clock	0.005mA	3.3V	0.0165mW
Sum: Nominal Operation	-	-	38.2mW
SD Card	28mA	3.3V	92.4mW
WIFI	190mA	3.3V	627mW
Sum: Maximum Peak	-	-	757.6mW

data in the vicinity of spin-down events are downloaded via WIFI. The raw data file received from the VAMPIRE is then checked to find specific signatures of the electromechanical system for mechanical failures by constructing an eVTF. The self-sustenance of the VAMPIRE can be verified by confirming its nominal operation while the motor is active and measuring the required minimum power for the VAMPIRE. The validity of the VAMPIRE as a digital-embedded system can be verified by constructing eVTFs with the sensor data acquired from the VAMPIRE and checking whether the eVTFs can indicate such signatures of mechanical failures.

B. Results—Operation and Power Consumption

In the experiment, the electromagnetic energy harvester successfully powered the entire embedded system and supported the nominal operation of the VAMPIRE. Except for the SD card writing and WIFI data transfers, both of which happen after spin-down events, the nominal operating power for the VAMPIRE is 38.2 mW. The average current consumption is approximately 9.55 mA at the supercapacitor voltage of 4.0 V. The breakdown of the power consumption within the VAMPIRE is described in Table III. The nominal operation includes harvester switchings for rectification, power maximization, power regulation, sampling all the sensors at 2 kHz, storing the sampled data into the FRAM block, and maintaining the BLE connection continuously. As the SD card with the integrated WIFI module needs at least 92.4 mW, even when idling, it is heavily power-gated. If a WIFI connection is established by user's request, it requires additional 627 mW, making the entire power consumption of the VAMPIRE reaching up to 757.6 mW.

The frequency of accessing the VAMPIRE through WIFI must be tightly controlled in order to guarantee nonnegative power flow into the energy buffer. For example, if the motor runs with 10 A_{RMS} with the minimum run-time of 10 min, the VAMPIRE can harvest approximately 120 mW for 10 min. Deducting the nominal operation power of approximately 40 mW, the remaining 80 mW can be stored in the energy buffer for 10 min. With this net positive energy stored,

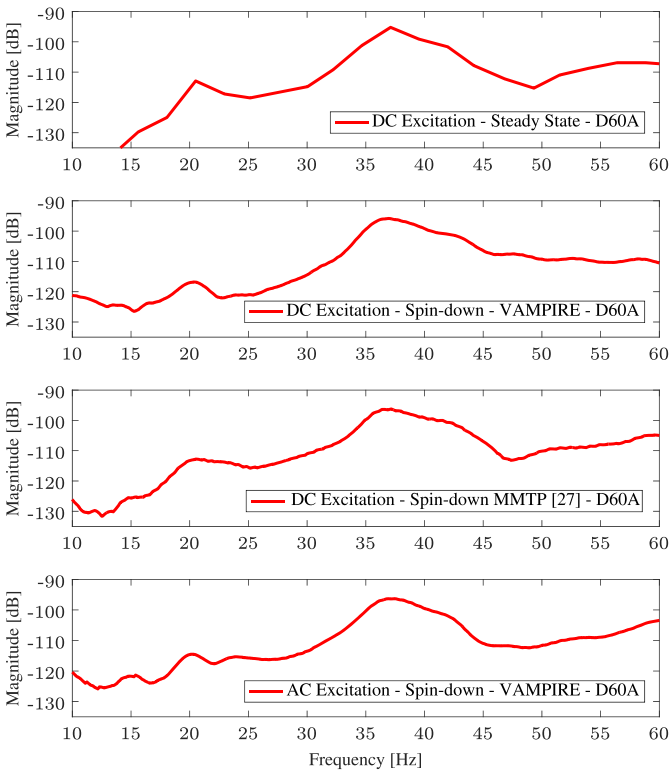

Fig. 12. Frequency response functions for the same mount system produced with four different methods for cross validation.

the maximum power dissipation of the VAMPIRE with the WIFI connection can be sustained for approximately 60 s.

However, a user can decide to drain the energy buffer extensively, beyond the nonnegative energy flow constraint. The user will require more time to charge it up in a later access if the user wants the VAMPIRE to be an independent self-powered embedded system again. In any case, the LiPo battery is still protected by the circuit such that it cannot be drained lower than 3.85 V as a precaution to maintain chemical stability and avoid a permanent damage to it. In the case of an interrupted wireless data transmission due to LiPo disconnection, the data can be retrieved in a later access as the data are stored in a nonvolatile space.

C. Results—Data Validity as an Embedded System

A series of eVTFs are generated using the signal processing algorithm introduced in [27] with the sensor data acquired from the VAMPIRE.

First, in Fig. 12, the VAMPIRE is cross-validated against existing methods, namely, a steady-state analysis and a spin-down analysis using existing equipment of [27]. The first plot is generated by exciting the dc motor at multiple frequencies and collecting the steady-state vibration data. The second plot is generated from a spin-down event by the VAMPIRE powered by the energy buffer with the electromechanical structure excited by the dc motor. The third is generated from a spin-down event by the existing system, the motor mount test platform used in [27], which is illustrated in Fig. 13. The dc motor is excited in this case. The fourth plot is generated

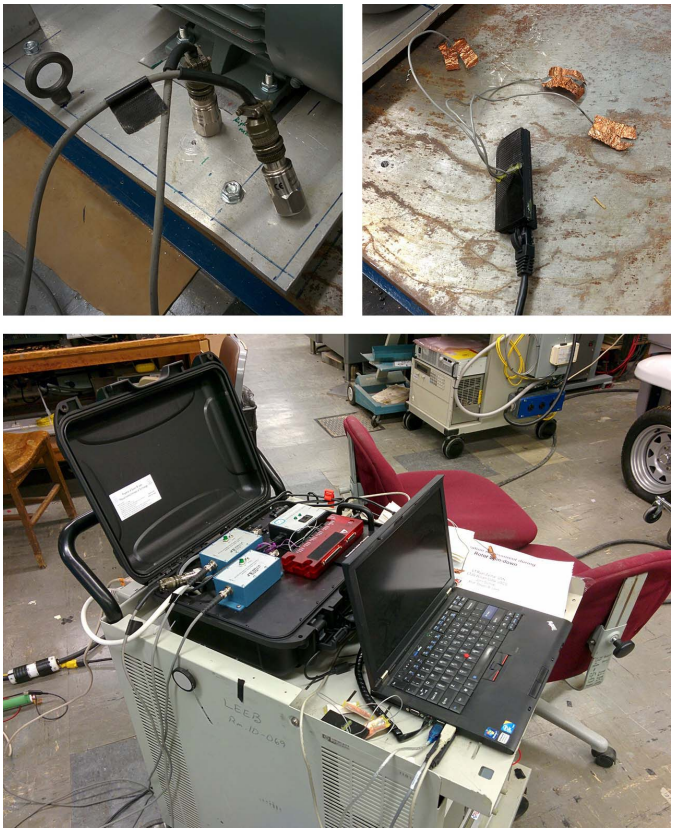

Fig. 13. Entire equipment set of [27] that VAMPIRE makes obsolete and replaces: commercial accelerometers (top left); standalone back-EMF sensors (top right); data acquisition blocks, data storage, data network, data wiring, power supply, and power wiring (bottom).

from a spin-down event by the VAMPIRE with the ac motor excitation, where the VAMPIRE is sustained by the internal energy harvester. The stiffness of the mounts used in these four cases is the same: durometer of 60 A. Also added is the load imbalance of 17 g to the shaft for these cases. With any excitation method, either the dc excitation or the ac excitation, the VAMPIRE provides an almost identical primary resonance location, compared with the steady state and the existing spin-down analysis method [27]. The overall shapes of the eVTFs that the VAMPIRE generate also agree well with the existing methods. All the four methods produce essentially similar results, providing confidence that the VAMPIRE hardware and algorithms are offering correct and reliable information for diagnostics. The different shapes of the spin-down results in the low-frequency region compared with the steady-state result are due to the fact that the rotor speed is low and can be easily affected by ambient noise. The different shapes at the higher frequency tail primarily derive from the different transient responses of ac and dc motors at the initiation of a spin-down event, coupled with misalignment of accelerometers' axes in different systems.

The primary peak area is zoomed in for a closer verification in Fig. 14. As shown in Fig. 14, the location of the peak, which is the one of the most important characteristics in an eVTF, matches accurately for every case. This implies that an eVTF generated by the VAMPIRE can identify the mechanical self-resonant frequency as accurate as other methods.

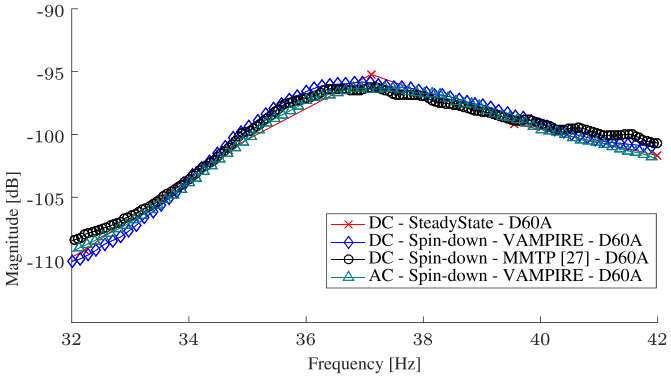

Fig. 14. Close-up view of the primary peaks of the vibration transfer functions produced by four different experimental methods: the close agreement of the four methods underscores the reliability of the VAMPIRE approach for producing quick eVTFs accurately during a spin-down experiment.

Second, VAMPIRE's capability to identify electromechanical pathologies is verified. Instead of the Hilbert transform, zero crossings are detected to estimate the rotor speed. Two different mounts with durometer of 40 and 60 A are assumed. At the same time, a load imbalance of 17 g is considered for each mount as well, giving a total of four cases. The locations of the mounts with changeable stiffness and the load imbalance are shown in Fig. 10, and the physical connection of the changeable mounts is illustrated in Fig. 11. The eVTF results are presented in Fig. 15. Consider the red curve, "D40A," as the base case. When the imbalance is added to the shaft, the coefficient C appearing in [27, eq. (4)], which is directly proportional to load mass and imbalances, is increased. Since the y-axis is in dB, the increased coefficient results in a vertical shift, as shown in the blue curve, "D40A Imbalance." When the D40A mounts are replaced with the D60A mounts (but still with the load imbalance), the change in the stiffness of the mounts results in different vibration dampening and brings the change in the mechanical self-resonant frequency. This clearly manifests as a horizontal shift, as shown in the green curve, "D60A Imbalance." When the load imbalance is removed with the D60A mounts, the vertical shift in the reverse direction happens as C is decreased, presenting the black curve, "D60A."

For all the cases in Figs. 14 and 15, each data point in a curve represents a single measurement. Curves constructed with averaged repeated measurements would be smoother and cleaner, especially in a noisy environment, due to elimination of high-frequency jitters and noises. However, averaging was not employed in this paper as each curve constructed from a single measurement was already sufficiently clean.

By monitoring changes in eVTFs over time, two separate electromechanical issues can be diagnosed: a change in mount stiffness and a change in load imbalance. A change in stiffness can imply a damaged or degraded mounts. A change in load imbalance can imply a damaged load, a changed load profile, or a damaged shaft axle. Heuristics to quantify the shape of an eVTF, for example, locations of the primary peaks and corresponding magnitudes, slopes at certain regions, and so on, can be implemented on a monitoring system with

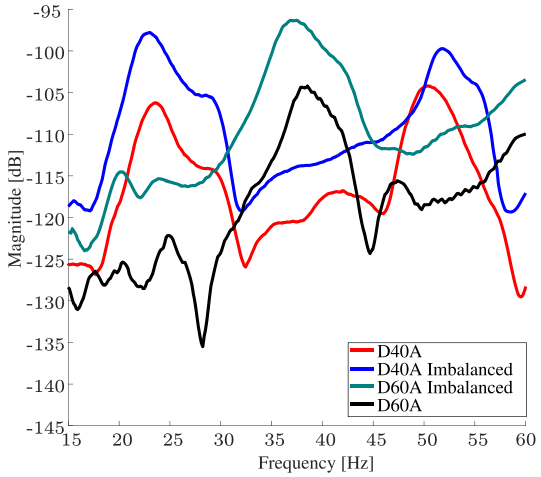

Fig. 15. Four experiments showing the shift of amplitude with imbalance and the shift of peak frequencies with changing mount stiffness.

a networking capability [30] and automatically generate an indication for users for condition-based maintenance, enabling failure prevention, and low-cost maintenance for the electromechanical systems.

Most importantly, the VAMPIRE can provide the same fidelity in results with a significantly smaller volume (5 cm × 5 cm × 1 cm), compared with the existing systems. The VAMPIRE can entirely replace the commercially available measurement setup of [27], illustrated in Fig. 13, which consists of standalone accelerometers and back-EMF sensors, data acquisition blocks, data storage, data network, data wiring, power supply, and power wiring. It also has an additional benefit of being nonintrusive as a sensor node.

VII. Conclusion

This paper presents the design of a self-powered embedded system that illustrates how magnetic harvesting can be managed for many different sensing applications, including thermal, voltage monitoring, speed monitoring, current sensing, and so on. The power flow and regulation stages in the power package are explored, and the necessity and implementation of an energy buffer are illustrated.

Multiple power paths are properly controlled to accommodate multiple power sources that require charging, discharging, and regulation. A spin-down event, which is crucial for electromechanical diagnosis, is detected using the inherent nature of a nonideal current transformer, detecting a sudden collapse of magnetic fields. The sensors and microcontrollers to acquire data are also discussed in detail. Two wireless communication protocols are employed in the design: BLE and WIFI. The BLE connection is used for issuing commands, checking the status of the embedded system, and configuring options. The WIFI connection is used for raw data transfers.

The VAMPIRE prototype has been built and verified for power and function. The system operates with 38.2-mW nominal power consumption, with the option of performing power-intensive operations, such as SD card writing and WIFI data transmission after spin-down events, provided that the energy buffer supplies the net-positive energy that it accumulated during the normal motor run time. The performance of VAMPIRE sensors is successfully validated against a steady-state analysis and a spin-down analysis using commercially available equipment. Also, a change in mount stiffness, which implies damaged or degraded mounts, and a change in load imbalance, which implies a damaged load, a changed load profile, or a damaged shaft axle, can be identified using the sensor data acquired from the VAMPIRE, enabling this process to be used for condition-based maintenance for electromechanical diagnosis. The VAMPIRE is significantly smaller in physical volume and can replace the commercially available setup, keeping the measurement accuracy unaffected.

Acknowledgment

The authors gratefully acknowledge the support of the MITei-ExxonMobil Program, the Office of Naval Research Structural Acoustics Program, and The Grainger Foundation.

References

[1] H. Zangl, T. Bretterklieber, and G. Brasseur, "A feasibility study on autonomous online condition monitoring of high-voltage overhead power lines," *IEEE Trans. Instrum. Meas.*, vol. 58, no. 5, pp. 1789–1796, May 2009.

[2] L. Hou and N. W. Bergmann, "Novel industrial wireless sensor networks for machine condition monitoring and fault diagnosis," *IEEE Trans. Instrum. Meas.*, vol. 61, no. 10, pp. 2787–2798, Oct. 2012.

[3] D. Sun *et al.*, "On-line nonintrusive detection of wood pellets in pneumatic conveying pipelines using vibration and acoustic sensors," *IEEE Trans. Instrum. Meas.*, vol. 63, no. 5, pp. 993–1001, May 2014.

[4] E. Sardini and M. Serpelloni, "Self-powered wireless sensor for air temperature and velocity measurements with energy harvesting capability," *IEEE Trans. Instrum. Meas.*, vol. 60, no. 5, pp. 1838–1844, May 2011.

[5] M. D. Prieto, D. Z. Millan, W. Wang, A. M. Ortiz, J. A. O. Redondo, and L. R. Martinez, "Self-powered wireless sensor applied to gear diagnosis based on acoustic emission," *IEEE Trans. Instrum. Meas.*, vol. 65, no. 1, pp. 15–24, Jan. 2016.

[6] J. J. Ruan, R. A. Lockhart, P. Janphuang, A. V. Quintero, D. Briand, and N. de Rooij, "An automatic test bench for complete characterization of vibration-energy harvesters," *IEEE Trans. Instrum. Meas.*, vol. 62, no. 11, pp. 2966–2973, Nov. 2013.

[7] F. Salvadori *et al.*, "Monitoring in industrial systems using wireless sensor network with dynamic power management," *IEEE Trans. Instrum. Meas.*, vol. 58, no. 9, pp. 3104–3111, Sep. 2009.

[8] J. P. Amaro, R. Cortesao, J. Landeck, and F. J. T. E. Ferreira, "Harvested power wireless sensor network solution for disaggregated current estimation in large buildings," *IEEE Trans. Instrum. Meas.*, vol. 64, no. 7, pp. 1847–1857, Jul. 2015.

[9] Z. Liu, D. S. Forsyth, J. P. Komorowski, K. Hanasaki, and T. Kirubarajan, "Survey: State of the art in NDE data fusion techniques," *IEEE Trans. Instrum. Meas.*, vol. 56, no. 6, pp. 2435–2451, Dec. 2007.

[10] H.-C. Lee, K.-H. Ke, Y.-M. Fang, B.-J. Lee, and T.-C. Chan, "Open-source wireless sensor system for long-term monitoring of slope movement," *IEEE Trans. Instrum. Meas.*, vol. 66, no. 4, pp. 767–776, Apr. 2017.

[11] Z. Wang, J. Hu, J. Han, G. Zhao, J. He, and S. X. Wang, "A novel high-performance energy harvester based on nonlinear resonance for scavenging power-frequency magnetic energy," *IEEE Trans. Ind. Electron.*, vol. 64, no. 8, pp. 6556–6564, Aug. 2017.

[12] T. Hosseinimehr and A. Tabesh, "Magnetic field energy harvesting from AC lines for powering wireless sensor nodes in smart grids," *IEEE Trans. Ind. Electron.*, vol. 63, no. 8, pp. 4947–4954, Aug. 2016.

[13] J. Han, J. Hu, Y. Yang, Z. Wang, S. X. Wang, and J. He, "A nonintrusive power supply design for self-powered sensor networks in the smart grid by scavenging energy from AC power line," *IEEE Trans. Ind. Electron.*, vol. 62, no. 7, pp. 4398–4407, Jul. 2015.

[14] M. Gao, P. Wang, Y. Cao, R. Chen, and D. Cai, "Design and verification of a rail-borne energy harvester for powering wireless sensor networks in the railway industry," *IEEE Trans. Intell. Transp. Syst.*, vol. 18, no. 6, pp. 1596–1609, Jun. 2017.

[15] S. Sudevalayam and P. Kulkarni, "Energy harvesting sensor nodes: Survey and implications," *IEEE Commun. Surveys Tuts.*, vol. 13, no. 3, pp. 443–461, 3rd Quart., 2011.
[16] L. Buccolini and M. Conti, "An energy harvester interface for self-powered wireless speed sensor," *IEEE Sensors J.*, vol. 17, no. 4, pp. 1097–1104, Feb. 2017.
[17] B. P. Nabar, Z. Celik-Butler, and D. P. Butler, "Self-powered tactile pressure sensors using ordered crystalline ZnO nanorods on flexible substrates toward robotic skin and garments," *IEEE Sensors J.*, vol. 15, no. 1, pp. 63–70, Jan. 2015.
[18] D. Lee, "Wireless and powerless sensing node system developed for monitoring motors," *Sensors*, vol. 8, no. 8, pp. 5005–5022, 2008.
[19] A. Tanaka, F. Utsunomiya, and T. Douseki, "Wearable self-powered diaper-shaped urinary-incontinence sensor suppressing response-time variation with 0.3 V start-up converter," *IEEE Sensors J.*, vol. 16, no. 10, pp. 3472–3479, May 2016.
[20] L.-C. Chang and D.-S. Lee, "The development of a monitoring system using a wireless and powerless sensing node deployed inside a spindle," *Sensors*, vol. 12, pp. 24–41, Dec. 2011.
[21] J. Moon and S. B. Leeb, "Enhancement on energy extraction from magnetic energy harvesters," in *Proc. IEEE Energy Convers. Congr. Expo. (ECCE)*, Sep. 2015, pp. 427–433.
[22] I. Stark, "Invited talk: Thermal energy harvesting with thermo life," in *Proc. IEEE Int. Workshop Wearable Implant. Body Sensor Netw.*, Apr. 2006, pp. 19–22.
[23] J. A. Paradiso and T. Starner, "Energy scavenging for mobile and wireless electronics," *IEEE Pervasive Comput.*, vol. 4, no. 1, pp. 18–27, Jan./Mar. 2005.
[24] J. Moon and S. B. Leeb, "Analysis model for magnetic energy harvesters," *IEEE Trans. Power Electron.*, vol. 30, no. 8, pp. 4302–4311, Aug. 2015.
[25] J. Moon and S. B. Leeb, "Power electronic circuits for magnetic energy harvesters," *IEEE Trans. Power Electron.*, vol. 31, no. 1, pp. 270–279, Jan. 2016.
[26] J. Moon and S. B. Leeb, "Power flow control and regulation circuits for magnetic energy harvesters," in *Proc. IEEE 15th Workshop Control Modeling Power Electron. (COMPEL)*, Jun. 2014, pp. 1–8.
[27] R. Zachar, P. Lindahl, J. Donnal, W. Cotta, C. Schantz, and S. B. Leeb, "Utilizing spin-down transients for vibration-based diagnostics of resiliently mounted machines," *IEEE Trans. Instrum. Meas.*, vol. 65, no. 7, pp. 1641–1650, Jul. 2016.
[28] J. Moon and S. B. Leeb, "Power loss analysis with high primary current in magnetic energy harvesters," in *Proc. IEEE 16th Workshop Control Modeling Power Electron. (COMPEL)*, Jul. 2015, pp. 1–8.
[29] J. S. Donnal and S. B. Leeb, "Noncontact power meter," *IEEE Sensors J.*, vol. 15, no. 2, pp. 1161–1169, Feb. 2015.
[30] J. Paris, J. S. Donnal, and S. B. Leeb, "NilmDB: The non-intrusive load monitor database," *IEEE Trans. Smart Grids*, vol. 5, no. 5, pp. 2459–2467, Sep. 2014.
[31] C. J. Schantz, "Methods for non-intrusive sensing and system monitoring," Ph.D. dissertation, Dept. Mech. Eng., Massachusetts Inst. Technol., Cambridge, MA, USA, 2014.
[32] Z. Tang, P. Pillay, and A. M. Omekanda, "Vibration prediction in switched reluctance motors with transfer function identification from shaker and force hammer tests," *IEEE Trans. Ind. Appl.*, vol. 39, no. 4, pp. 978–985, Jul. 2003.

Jinyeong Moon (S'12–M'16) received the B.S. degree in electrical engineering and computer science from the Korea Advanced Institute of Science and Technology, Daejeon, South Korea, in 2005, the M.S. degree in electrical engineering from Stanford University, Stanford, CA, USA, in 2007, and the Ph.D. degree in electrical engineering and computer science from the Massachusetts Institute of Technology (MIT), Cambridge, MA, USA, in 2016.

He was with Hynix Semiconductor Inc., Icheon, South Korea, from 2007 to 2011 as a Senior Research Engineer, where he was involved in designing analog, digital, and power circuits for DDR4 SDRAM. He was a postdoctoral associate at MIT from 2016 to 2017. He is currently with Maxim Integrated, North Chelmsford, MA, USA. He holds 17 registered U.S. and international patents. His current research interests include modeling, design, analysis, and measurement of circuits and systems in the fields of power conversion, energy harvesting, electromagnetics, and renewable energy.

Dr. Moon received the grand prize in the MIT Clean Energy Prize in 2014. He was also a recipient of the Kwanjeong Scholarship and the Hynix Strategic Patent Award.

Steven B. Leeb (S'89–M'91–SM'01–F'07) received the Ph.D. degree from the Massachusetts Institute of Technology (MIT), Cambridge, MA, USA, in 1993.

He has served as a Commissioned Officer with the United States Air Force, Washington, DC, USA. He has been a member of the MIT Faculty, Department of Electrical Engineering and Computer Science, MIT, since 1993. He also holds a joint appointment with the Department of Mechanical Engineering, MIT. He currently serves as a MacVicar Fellow and a Professor of electrical engineering and computer science with the Laboratory of Electromagnetic and Electronic Systems, MIT, where he is involved in the design, development, and maintenance processes for all kinds of machinery with electrical actuators, sensors, or power electronic drives. He has authored or co-authored over 100 publications. He holds 15 U.S. patents in the fields of electromechanics and power electronics.